

Cyclochiral conformers of resorcin[4]arenes stabilized by hydrogen bonds†

Agnieszka Szumna*

Received 30th January 2007, Accepted 7th March 2007

First published as an Advance Article on the web 23rd March 2007

DOI: 10.1039/b701451a

Cyclochiral resorcinarenes, that maintain their cyclochirality by means of hydrogen bonds, were synthesized by a sequence of reactions involving the Mannich reaction, removal of the *N,O*-acetal bridge and subsequent *N*-substitution with an RCO group. During this study it was found that ethyl nitroacetate is a mild and very efficient agent for *N,O*-acetal bridge removal. The resulting resorcinarenes **4a–j** exist in cyclochiral/inherently chiral kite conformations (resembling 4-bladed propellers) that are stabilized by eight hydrogen bonds (in both solid state and solution). It is shown that the cycloisomerization process is characterized by the relatively high racemization barrier (14.6–18.5 kcal mol⁻¹ as determined by 2D EXSY) and thus it can be concluded that the transformation of one cycloconformer into the other requires the simultaneous rupture of all eight hydrogen bonds. For derivatives with additional stereogenic centers two cyclodiastereoisomeric conformations were detected (diastereomeric excess in the range of 72% up to >95%). The experimental results are additionally supported by AM1 semi-empirical calculations.

Introduction

For the construction of chiral ligands for a variety of applications (including catalysis, separation, recognition and detection) the use of stereogenic centers as sources of chirality is a classical and still dominant approach. However, recently other types of chirality like axial^{1,2} or planar³ have also gained increasing importance. Not long ago the first application of molecules possessing so called 'inherent chirality' or 'cyclochirality' was reported.^{4,5} These types of chirality are dependent upon the curvature of the molecules. Inherent chirality derives from curvature of molecules that are devoid of symmetry axes in their bi-dimensional representation.⁶ The other similar term—cyclochirality—has been defined for

compounds made of the same building blocks that differ only in the sense of direction of the ring.^{7,8} Although, according to strict definitions, these two terms do not overlap, in the literature for some types of compounds the terms have been used interchangeably. For the purpose of this paper the term cyclochirality will be used as the one that is more in keeping with the phenomenon that is discussed.

The calix[*n*]arene skeleton is well suited for the construction of cyclochiral/inherently chiral molecules due to its immanent curvature that can be preserved. Several classes of calixarenes possessing these types of chirality have been reported. They involve calix[4]arenes with either a WXYZ or XXYZ substitution pattern at the upper rim, **I**,⁹ or cyclochirally substituted resorcin[4]arenes, **II** and **III** (Chart 1).^{10,11} The attractiveness of the last two types of compounds lies in the relative easy synthesis (using the Mannich reaction) and resolution as compared with substituted calixarenes **I**. The cyclochiral rim of intramolecular hydrogen bonds in resorcinarenes **II** and **III** drives the Mannich reaction to one regioisomer only and in the case of using chiral amine often to a

Institute of Organic Chemistry, Polish Academy of Sciences, Kasprzaka 44/52, 01-224, Warsaw, Poland. E-mail: szumnaa@icho.edu.pl; Fax: +48 22 632 6681; Tel: +48 22 343 2110

† Electronic supplementary information (ESI) available: crystallographic data for **4j** in CIF format, NMR spectra (PDF) and AM1 optimized structures in ML2 format. See DOI: 10.1039/b701451a

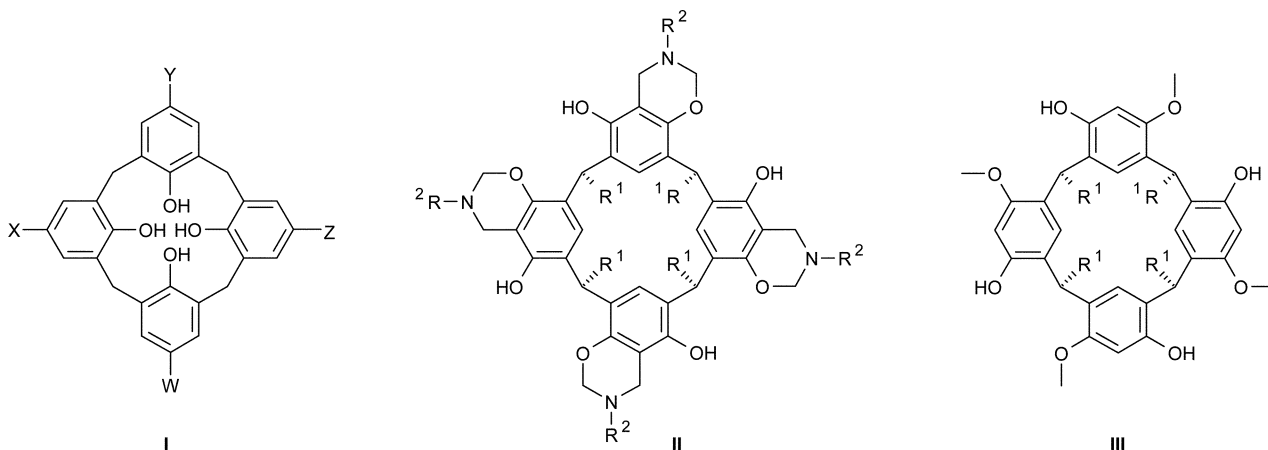


Chart 1 Examples of cyclochiral/inherently chiral calix[4]arenes.

single diastereoisomer.¹² Unfortunately, simple Mannich products **II** suffer from instability due to facile epimerization at the *N,O*-acetal bridge.¹³ The stability problem has been overcome for compounds of type **III**.

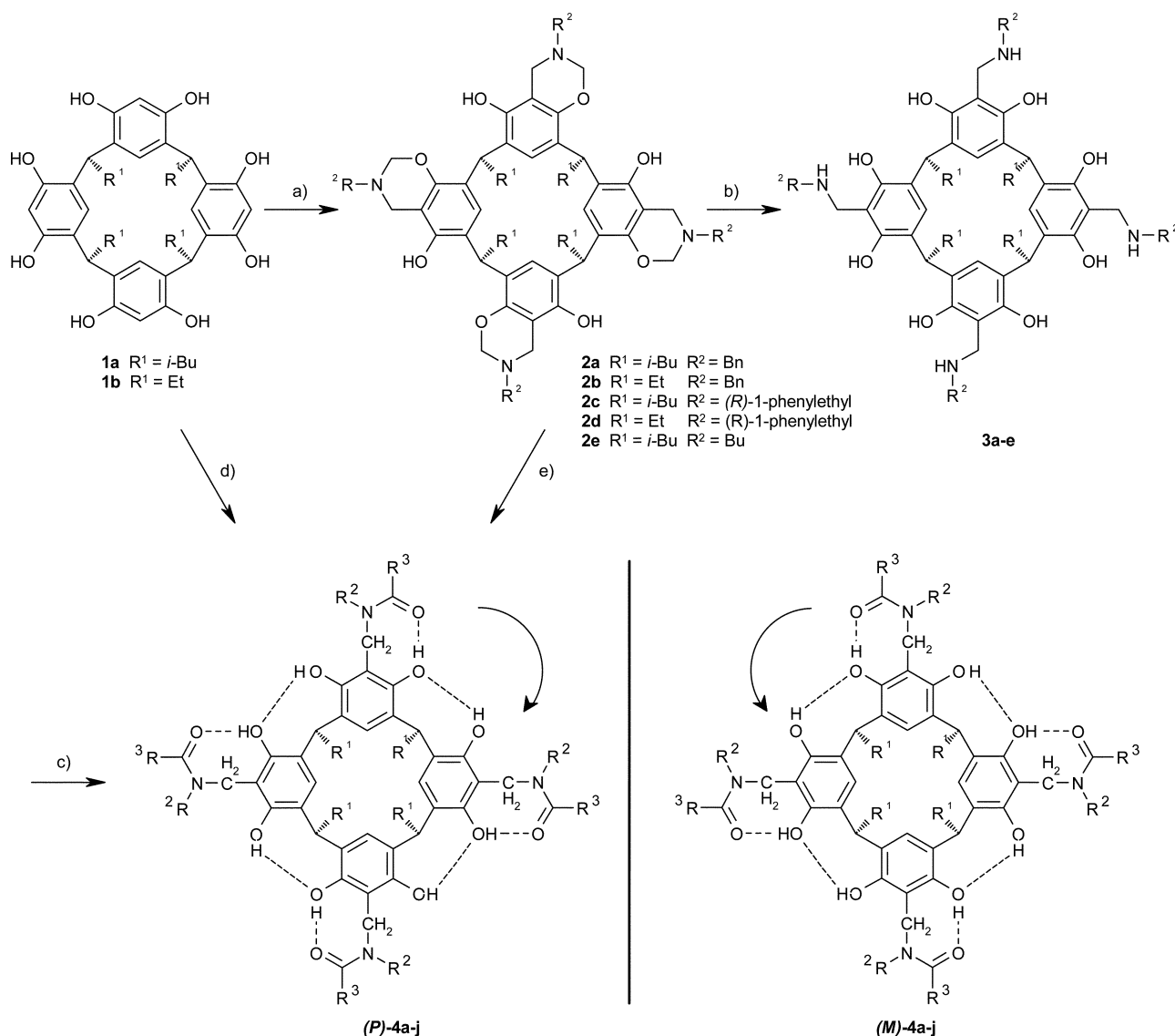
The current paper deals with cyclochiral compounds in which cyclochirality is of non-covalent origin. The synthesis, structure and stability of conformationally cyclochiral resorcinarenes **4** (Scheme 1) that maintain their cyclochirality by means of hydrogen bonds will be discussed. Additionally it will be shown that even though the cyclochirality is based on non-covalent interactions considerable diastereomeric excess can be detected.

While the conformational cycloenantiomerism of sterically interlocked molecules has attracted attention for decades, examples of similar phenomena based on hydrogen bonds are limited. Early examples were reported by the group of Rebek.¹⁴⁻¹⁶ They created deep cavitands with “doors” at the upper rim that were controlled

by a directional cooperative belt of hydrogen bonds, formed between the amide or hydroxy groups. For cyclodiastereomeric compounds diastereomeric excess was observed (d.e. 50%).

Another example involves an upper rim octaurea-functionalized resorcinarene, for which the existence of the cyclochiral belt of eight hydrogen bonds has been postulated.¹⁷ Calix[4]arene substituted at the lower rim by amino acids was also postulated to form a cyclochiral cooperative belt of four hydrogen bonds.¹⁸

Another interesting example, reported by Schmidt *et al.*,¹⁹ is actually a prototype of the system studied in this paper. Authors reported on the accidental synthesis of the *N*-acetyl derivative of the Mannich product obtained from an amine and tetraethylresorcin[4]arene. It was noticed that two distinct hydroxyl groups were observed by NMR which was indicative of cyclochiral conformation (as will be discussed later). However, no detailed conformational or stability studies were performed for this system.



Scheme 1 Synthesis of conformationally cyclochiral resorcinarenes: (a) amine, HCHO_{aq}, AcOH, MeOH; (b) ethyl nitroacetate, MeOH, rt, 2 h; (c),(d),(e) see Table 1 and Experimental section.

Results and discussion

Synthesis

In the current study I have synthesized resorcinarenes with acetyl (Ac), *tert*-butoxycarbonyl (Boc) and *tert*-butylaminocarbonyl (Bac) substituents on the nitrogen atom (Scheme 1). Tetralkyl resorcinarenes **1a–b** were transformed into tetrabenzoxazines **2a–d** by the Mannich reaction of **1a–b** with formaldehyde and benzylamine or (*R*)-1-phenylethylamine in methanol using a known procedure.^{10,12} The desired products **2a–d** precipitated from the reaction mixture and were isolated in high yields. While in the work by Böhmer,¹⁹ the *N*-acetylation of tetrabenzoxazines was achieved by chance and in moderate yield (18%), I have sought an efficient and general method for the *N*-substitution of tetrabenzoxazines **2a–d**. It seemed reasonable to cleave the *N,O*-acetal bridge first and then perform the *N*-substitution reaction. The known method for *N,O*-acetal removal involves using HCl in butanol (reflux). Such a method is efficient but it cannot be considered mild. During the course of this work it was found that ethyl nitroacetate reacts with tetrabenzoxazines **2a–d** with removal of the *N,O*-acetal bridge (the reaction was completed after *ca.* 2 h in methanol at room temperature). Additionally, it produces free amines **3a–d** and thus does not require using a base at the next stage (which could have caused undesired *O*-substitution). In all cases careful isolation and purification of free amines **3a–d** from the reaction mixture was not required. Thus the yields of **4a–j** given in Table 1 are for the two steps b and c.

The *tert*-butoxycarbonyl substituent was introduced using two different procedures. The convenient general procedure involves addition of Boc₂O to the crude reaction mixture containing amines **3a–e** in methanol affording precipitates, which upon recrystallization from CH₂Cl₂–MeCN gave analytically pure compounds **4a–e** in high yield (*e.g.* in the case of **4b** in 99% yield, Table 1, entry 5). The reaction could be also carried out “on water” (Table 1 entry 4). In this case, the reaction mixture containing **3b** had to be evaporated prior the addition of water and Boc₂O. Such a green approach was earlier reported to produce selectivity of the amino over phenol/alcohol Boc protection of amino acids and other simple amines.²⁰ Using this approach the desired product **4b** was obtained in 85% yield (Table 1, entry 4). Although this method is “green” it is far less convenient at the lab scale due to the requirement of hand-grinding of the reaction mixture.

The *tert*-butylaminocarbonyl substituent was introduced using *tert*-butyl isocyanate. The reaction required a coarse purification of the crude reaction mixture containing **3a–e** by washing with hexane and vacuum drying. The resulting oil was dissolved in THF and treated with *tert*-butyl isocyanate. Products **4f–j** were isolated by column chromatography.

The direct pathway, without removal of the aminoacetal bridge (Scheme 1, pathway e), was also studied. Two procedures were examined: direct reaction in THF and a two-phase reaction CH₂Cl₂/water. While for acetyl derivatives under two-phase conditions (CH₂Cl₂/water, Table 1, entry 3) route e gave the desired product **4a** in reasonable yield, for other derivatives (Boc and Bac) no products were observed. The other direct pathway (Scheme 1, route d), *i.e.* the Mannich reaction of *N*-Boc protected amines and formaldehyde with resorcinarenes **1a,b**, was also pursued. It did not give products either.

All products **4a–j** obtained in such a way have selectively substituted four N atoms, while the remaining hydroxy groups remain unsubstituted. For compounds that have eight OH and four amide groups the products are surprisingly non-polar. For example they are soluble in hexane, while they usually precipitate from MeOH, MeCN or even DMF and DMSO. This allows the assumption that for all products polar groups are engaged in intramolecular hydrogen bonding interactions, most probably following the pattern that was reported by Böhmer.¹⁹

X-Ray structure

The X-ray structure of compound **4j** confirmed an extensive intramolecular hydrogen-bonding pattern (Fig. 1). The molecule of **4j** has C₄ symmetry (both molecular and crystallographic) and adopts a *cyclochiral kite* conformation that is stabilized by the presence of eight hydrogen bonds. The most characteristic feature of this structure is the presence of four eight-membered hydrogen bonded rings that can bond concurrently in only one direction and thus are responsible for the existence of cyclochiral conformation. Within the eight-membered ring the strong hydrogen bonds are formed between the phenolic –OH and the amide C=O (distances: O8···O13 2.58 Å, H8···O13 1.78 Å, angle O8–H8···O13 154°). Outside the ring the same phenolic –OH group act as a hydrogen bond acceptor for the next slightly longer interaction with the neighbouring phenolic –OH (distances: O9···O8 2.70 Å, H9···O8 2.07 Å, angle O9–H9···O8 132°).

Table 1 Synthesis of cyclochiral resorcin[4]arenes **4** (Scheme 1)

Entry	Product	R ¹	R ²	R ³	(Steps) Conditions	Yield (%)
1	4a	<i>i</i> -Bu	Bn	methyl	(c) MeOH	56
2					(c) THF	21
3					(e) water/CH ₂ Cl ₂	43
4	4b	<i>i</i> -Bu	Bn	<i>tert</i> -butoxy	(c) water	85
5					(c) MeOH	99
6	4c	<i>i</i> -Bu	<i>n</i> -Bu	<i>tert</i> -butoxy	(c) MeOH	61
8	4d	<i>i</i> -Bu	(<i>R</i>)-1-phenylethyl	<i>tert</i> -butoxy	(c) MeOH	56
9	4e	Et	(<i>R</i>)-1-phenylethyl	<i>tert</i> -butoxy	(c) MeOH	56
10	4f	<i>i</i> -Bu	Bn	<i>tert</i> -butylamino	(c) THF	63
11	4g	Et	Bn	<i>tert</i> -butylamino	(c) THF	25
12	4h	<i>i</i> -Bu	<i>n</i> -Bu	<i>tert</i> -butylamino	(c) THF	54
13	4i	<i>i</i> -Bu	(<i>R</i>)-1-phenylethyl	<i>tert</i> -butylamino	(c) THF	48
14	4j	Et	(<i>R</i>)-1-phenylethyl	<i>tert</i> -butylamino	(c) THF	30

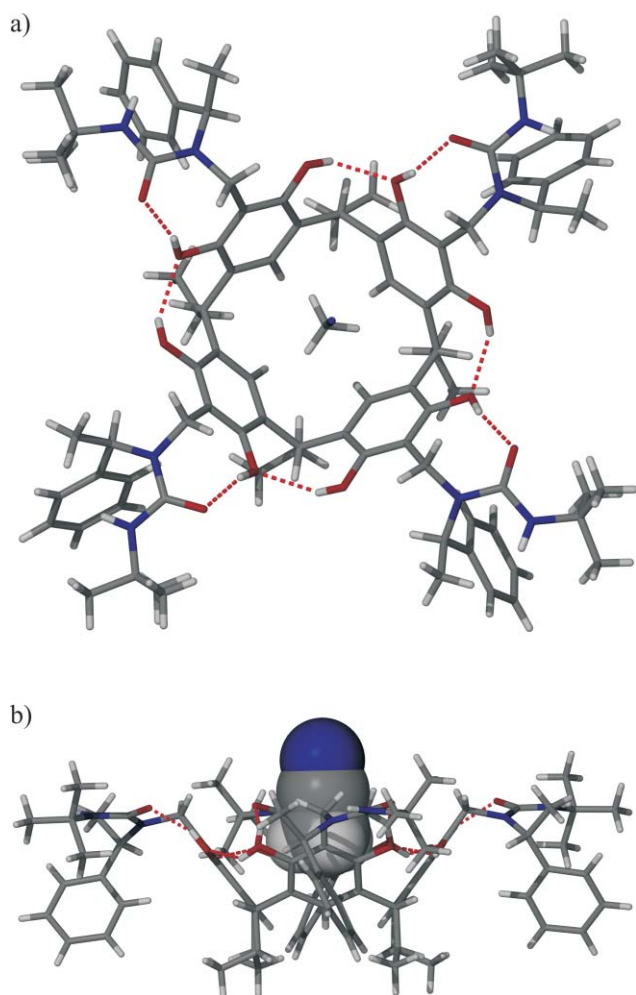


Fig. 1 The X-ray structure of (*M*)-(*R*)-**4j**: a) top view; b) side view. An acetonitrile (66%) or methanol (34%, not shown) molecule occupies the cavity.

Since the molecule contains additional known stereogenic centers ((*R*)-1-phenylethylamine fragments), the cyclochirality of **4j** can be determined unambiguously by the direction of the eight-membered hydrogen bonded ring closure. Assuming that: (a) the lower rim of the resorcin[4]arene **4j** is the bottom of the molecule, (b) looking from within the cavity, and (c) assuming priority of the –OH group hydrogen-bonded to the carbonyl oxygen atom over the –OH group hydrogen-bonded to the phenolic oxygen atom, the direction of ring closures can be described as *anticlockwise* or *M* (denoted as (*M*)-(*R*)-**4j**). It should be noted at this point that there is no uniform notation for the stereochemistry of cycloisomers of that type. Although it seems that an approach of looking from *within* the cavity is more spread out, an alternative view by looking from *above* the resorcinarene ring has recently been proposed but gives the opposite result.²¹ In this paper the convention of looking from within the cavity is used uniformly.

The other important feature of this structure is that the amide hydrogen atom is in close proximity to the aromatic ring (as was also deduced from NMR spectra, see next section). However the amide proton is not forming a N–H··· π interaction but instead points into a void formed by the methyl group and the phenyl ring. Despite this, the amide N–H remains quite shielded from the

environment, which manifests in its small temperature coefficient ($\Delta\delta/\Delta T$ 4.7×10^{-4} ppm K⁻¹) in NMR experiments.

It could be envisioned that the epimerization of such a system (to give a second cyclo-diastereoisomer) would be difficult, since the inversion at one ring only would have to disturb the entire belt of hydrogen bonded atoms and cause unfavourable interactions. This should cause a considerable kinetic stability for the conformers (*i.e.* high barriers to cycloepimerization).

NMR studies

Room temperature studies. For all products **4a–j** ¹H and ¹³C NMR spectra in CDCl₃ and toluene-*d*₈ exhibit a reduced number of signals in accordance with the C₄ symmetry of the molecules. In all cases two different signals for –OH protons were observed with a large chemical shift difference (*i.e.* one at *ca.* 8.9 ppm and the second one in the range of 11.5–12.8 ppm). The existence of two distinct –OH groups indicates that the molecules exist in relatively stable (exchange is slow on the NMR timescale) cyclochiral conformations with overall C₄ symmetry not only in the solid state but also in solution. The chemical shifts of those protons are considerably downfield shifted and concentration independent. This suggests that the intramolecular hydrogen bonding pattern observed in the solid state is most probably also maintained in solution.

Compounds **4a–c** and **4f–h**, devoid of other types of chirality, exist in the solution as mixtures of (*P*)- and (*M*)-cycloenantiomeric conformations (see Scheme 1). However, for compounds with additional stereocenters **4d–e** and **4i–j**, two cyclo-diastereoisomers (*P*)-(*R*)- and (*M*)-(*R*)-can be expected having most probably different spectra and unequal populations.

In fact for (*R*)-1-phenylethylamine-Bac derivatives **4i** and **4j** two sets of signals can be extracted from ¹H and ¹³C NMR spectra in toluene-*d*₈ and in CDCl₃ with a ratio of 0.86 : 0.14 (*d.e.* 72%). This transforms into 1.1 kcal mol⁻¹ difference in stability of the cycloconformers. The NOESY and ROESY spectrum of **4i** (see ESI†) shows the presence of cross-peaks between two diastereotopic methylene protons and the methine proton at the stereogenic centre: H_i ↔ H_e and H_f ↔ H_e (Fig. 2, see also ESI†). This may indicate that this proton is directed toward the upper side of the molecule (the opposite to what was observed in the solid state). The spectrum also shows the weak cross-peaks between the amide NH and all protons of the neighbouring

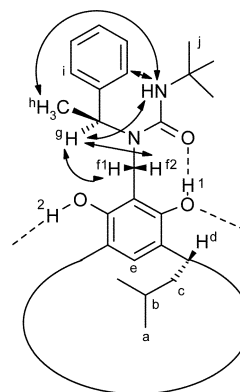


Fig. 2 Relevant ROESY contacts for major cycloconformer of **4i** (cycloconformation is ascribed arbitrarily).

(*R*)-1-phenylethylamine part: $\text{NH} \leftrightarrow \text{H}_g$, $\text{NH} \leftrightarrow \text{H}_h$, $\text{NH} \leftrightarrow \text{H}_i$ (Fig. 2, see also ESI†). This is due to the flexibility of (*R*)-phenylethylamine and unfortunately prevents unambiguous determination of the relative configuration of the cycloconformer.

For *tert*-butoxycarbonyl compounds **4d** and **4e**, possessing also central chirality, only one set of signals in the spectra can be found which implies that either: 1) one diastereoconformer is formed predominately (d.e. >95%); or 2) the exchange is dramatically faster than for other compounds; or 3) signals accidentally overlap. The dramatically faster exchange seems to be unlikely since two OH signals are still visible. An accidental overlap of signals cannot be excluded unambiguously, however it should be noted that for **4e** signals are relatively sharp (even sharper than for **4j** and scalar splitting, e.g. for AB systems, can be seen clearly). Additionally, the ^{13}C NMR spectrum shows one set of signals (see ESI†) and thus the accidental overlap of signals also appears to be unlikely. Thus, for **4e** it can be postulated that a single cyclodiastereoconformer exists predominately (d.e. >95%) in CDCl_3 solution at 303 K. The NOESY spectrum of **4e** shows the presence of weak cross-peaks between diastereotopic methylene $\text{H}_f \leftrightarrow \text{H}_i$ (aromatic), $\text{H}_f \leftrightarrow \text{H}_h$ (methyl protons) and $\text{H}_f \leftrightarrow \text{H}_g$ (methine) (Fig. 3). This is due to partially free rotation of the (*R*)-phenylethylamine group and unfortunately prevents the determination of the relative configuration of the cycloconformer.

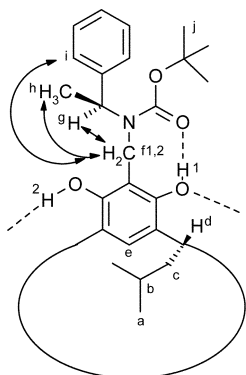


Fig. 3 Relevant NOESY contacts for **4e** (cycloconformation is ascribed arbitrarily).

Kinetic studies. The process of racemization between two cycloconformers involves an exchange between distinct hydroxy protons. The rates of exchange transform directly into racemization barriers, which can be used as measures of the relative tendency of molecules to maintain their intramolecular hydrogen bonding and thus their cyclochiral conformation. The exchange process was studied using variable temperature measurements and 2D EXSY.

The variable temperature measurements were performed in toluene- d_8 for **4b–d**, **4f** and **4i**. To minimize experimental errors the experiment was conducted so that the whole set of samples was recorded at the same time at a given temperature after stabilization.† For signals of protons in a slow to intermediate exchange regime (on the NMR timescale) it is expected that increasing the temperature would speed up the exchange and

thus would result in signal broadening and finally coalescence. The shape analysis of the variable temperature NMR spectra (VT NMR) should thus give the rates of exchange. However, in this case the VT NMR spectra (303–373 K interval) show that increasing the temperature causes the half-widths of the OH signals to first slightly decrease and then increase (Fig. 4). Additionally it was observed that at room temperature the half-widths of the OH signals are strongly magnetic field dependent.§ Such behavior can be explained if one assumes that at room temperature each cycloconformer is in fast equilibrium with a set of its low-abundance conformers which derive from breaking of individual hydrogen bonds (one or more), however, without significant structure rearrangement. At room temperature the exchange by “individual hydrogen bond rupture” is relatively faster than the exchange by “racemization” and thus the former contributes mainly to the line broadening. As the temperature increases, the exchange by “individual hydrogen bond rupture” becomes very fast, while the exchange by “racemization” reaches the region of intermediate rates and thus is the main contributor to the line broadening.

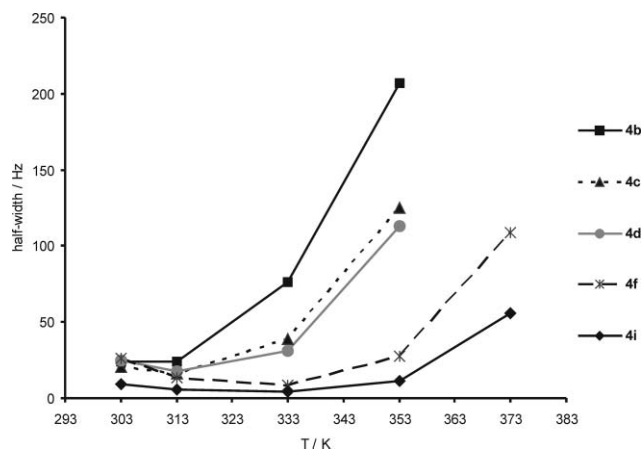


Fig. 4 Temperature dependence of half-width of OH signals (average of two OH signals).

Due to the additional co-existing process (being in the regime of fast exchange) it is difficult to extract kinetic data from these measurements. However some qualitative conclusions can still be elucidated, especially from the high temperature data (Fig. 4). From the data, it is worth noting that compounds **4b–d** having *tert*-butoxycarbonyl substituents reach coalescence at ca. 365 K, while *tert*-butylaminocarbonyl derivatives **4f** and **4i** do not reach coalescence up to 373 K. Additionally the half-widths of signals for *tert*-butylaminocarbonyl derivatives (which is directly proportional to the exchange rate) at a given temperature (e.g. 353 K) are considerably lower than for their *tert*-butoxycarbonyl counterparts (**4b** vs. **4f** and **4d** vs. **4i**). This means that compounds having NH atoms instead of an oxygen atom have more stable cycloconformations. This may be attributed to the bulkiness of the NH group compared with the oxygen atom and/or favourable interactions of NH with the neighbouring aromatic ring as compared with the probably repulsive interaction between an

† It has been checked experimentally that this method produces less experimental errors than measuring each sample separately.

§ For example for **4b** the half-width of OH signals are 10 Hz on 200 MHz NMR and 40 Hz on 400 MHz NMR at 295 K.

oxygen atom and an aromatic ring. The proximity of NH atoms to the benzylamine aromatic ring is also supported by the X-ray structure and by the chemical shift of the NH protons, which show up at 3.94 ppm for **4i** (assignment based on ^1H - ^{15}N HSQC spectrum). Such an upfield shift is most probably due to shielding caused by the neighboring aromatic ring. Steric hindrance at the benzylamine part also has a pronounced, though smaller, positive effect on the stability (*i.e.* compare derivatives of (*R*)-1-phenylethylamine **4d** and **4i** with their respective benzylamine analogues **4b** and **4f**).

The exchange process for **4i** ((*R*)-phenylethylamine-Bac derivative) was observed using 2D EXSY spectroscopy. In this case racemization of the cyclic array of hydrogen bond produces a second diastereoconformer, and thus the exchange process should take place between the two cycloconformers. The existence of separate signals for two diastereoconformers is a lucky situation since it allows for elimination of NOE effects, which are otherwise difficult to separate. The exchange correlation cross-peaks appear between signals of different cycloconformers (Fig. 5). The basis for the extraction of kinetic data is integration of the cross-peak volumes in the 2D EXSY NMR spectra.²² The exchange rate, calculated using integration of signals from different protons undergoing exchange in **4i** (OH, NH and aliphatic), was found to be $k = 1.9 \pm 0.3 \text{ s}^{-1}$ at 303 K in CDCl_3 . It should be noted that at optimal temperatures (high temperature range to

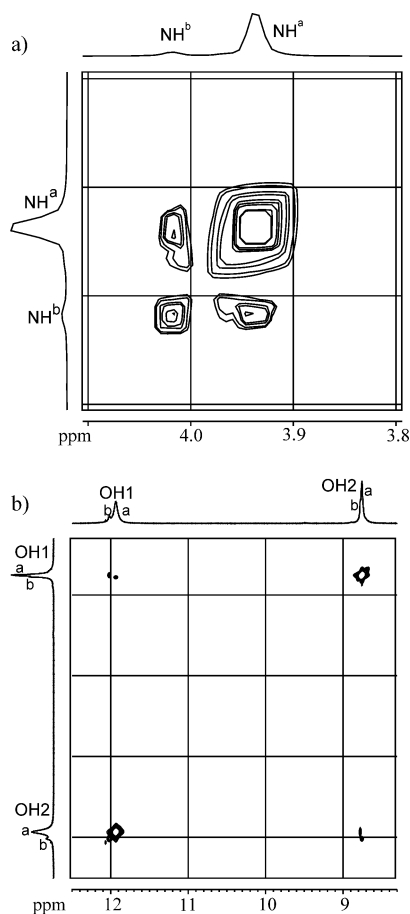


Fig. 5 2D EXSY spectrum of **4i**: a, major cycloconformer; b, minor cycloconformer (CDCl_3 , 500 MHz, 303 K, $\tau_m = 250 \text{ ms}$). a) Amide NH region; b) OH region.

minimize errors caused by co-existing exchange) the extracted rate constants from variable temperature spectra and extrapolated to 303 K give $k = 1.0 \text{ s}^{-1}$ in toluene- d_8 which is in surprisingly good agreement, with those obtained from the EXSY spectrum. The rate constant $k = k_1 + k_{-1} = 1.9 \text{ s}^{-1}$ for an 0.86 : 0.14 conformer ratio translates to exchange barriers of $\Delta G^\ddagger = 18.5 \text{ kcal mol}^{-1}$ (major \rightarrow minor) and $17.4 \text{ kcal mol}^{-1}$ (minor \rightarrow major) at 303 K in CDCl_3 . Those are quite reasonable values for the cost of rupturing simultaneously eight hydrogen bonds. The typical costs of hydrogen bond rupture in organic solvents is roughly 1 to 2 kcal mol^{-1} per hydrogen bond.²³ In fact for the breaking of eight coherent hydrogen bonds in cavitands a barrier of $17.4 \text{ kcal mol}^{-1}$ was observed. However, it should be noted that in the previous case the hydrogen bonds are arranged in a cooperative seam (*i.e.* one amide group that is a donor of hydrogen bond simultaneously acts as an acceptor for the next bond). In contrast this system has a hydrogen bond system that is spatially separated and divided into four parts, which are interlocked by rotation. It is also important to note that the existence of a cooperative seam of eight hydrogen bonds is not enough for the considerable kinetic stability of cycloconformers (*e.g.* octaurea-functionalized resorcinarenes reveal rapid interconversion between conformers).

The 2D EXSY spectrum of **4e** ((*R*)-phenylethylamine-Boc derivative) shows the exchange cross-peaks only between the two different OH groups (in two spectra that used different mixing times $\tau_m = 20 \text{ ms}$ and $\tau_m = 250 \text{ ms}$, Fig. 6). The exchange process that leads to entities that are indistinguishable from the starting molecules has the disadvantage that the exchange intensity data can be strongly biased by NOE (OH protons are in close proximity). To avoid this the kinetic data were extracted from the EXSY spectrum using a short mixing time $\tau_m = 20 \text{ ms}$. A short mixing time causes the NOEs to be negligible and fortunately the intensities of the exchange cross-peaks were reasonably high. However, the inability to observe the second diastereoconformer raises the question about interpretation of kinetic data, since the conversion to the identical cycloconformer, observed in the NMR experiment, requires two rotation steps (*i.e.* (*M*)-(*R*)-**4e** \rightarrow (*P*)-(*R*)-**4e** \rightarrow (*M*)-(*R*)-**4e**). Additionally calculation of rate constants from the EXSY spectrum requires knowledge of the mole fractions, so the assumption of the ratio of diastereoconformers

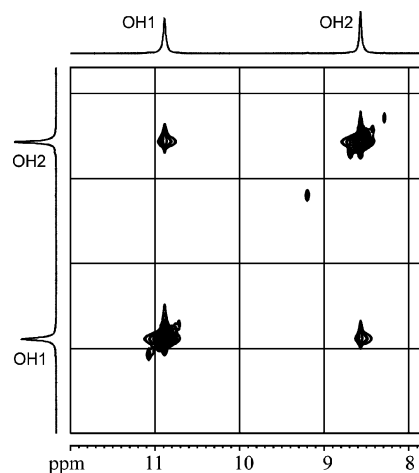


Fig. 6 2D EXSY spectrum of **4e** (CDCl_3 , 500 MHz, 303 K, $\tau_m = 20 \text{ ms}$); OH protons region.

has to be made prior to the calculations. Since the exchange is visible, the second diastereconformer has to exist in a detectable amount. However, its signals would have: (1) lower intensity and (2) larger half-width due to faster exchange and thus might not be visible. Based on the condition d.e. $\sim 95\%$ and on the calculation mathematical limits the assumption of a 0.976 : 0.026 conformer ratio was made. The exchange rate was calculated to be $k = k_1 + k_{-1} = 195.2 \text{ s}^{-1}$ at 303 K, which transforms into interconversion barriers of $16.7 \text{ kcal mol}^{-1}$ (major \rightarrow minor) and $14.6 \text{ kcal mol}^{-1}$ (minor \rightarrow major) at 303 K in CDCl_3 .

CD spectra

Circular dichroism spectroscopy provides further evidence for the existence of stable cyclo-diastereconformers. Fig. 7 show the CD spectra of **4d**, **4e**, **4i**, and **4j**. The existence of pronounced, though not very strong (as compared with other “covalently” cyclochiral resorcinarenes)²⁴ Cotton effects of opposite signs was observed for the absorption bands at 291 and 310 nm, which are attributed to electronic transitions of the resorcinol chromophore. It indicates that even though the stereogenic centers are quite remote, the parent resorcinarene ring still experiences a chiral environment. This is probably due to the cyclochiral arrangement of hydrogen bonds. In fact, Cotton effects caused by cyclochiral conformation have been reported previously for octaurea-substituted resorcinarenes.

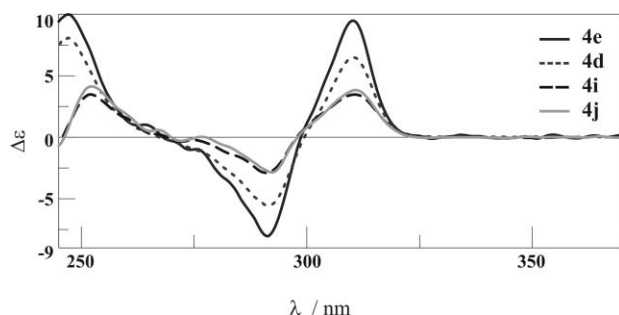


Fig. 7 CD spectra of cyclochiral resorcinarenes (CHCl_3 , 295 K).

Based on the similarity of the CD spectra (Fig. 7), it can be speculated that in all cases the same cycloconformer is predominant. The larger values of $\Delta\epsilon$ for *tert*-butoxycarbonyl derivatives as compared with *tert*-butylaminocarbonyl derivatives may also indicate that in the former case, the diastereomeric excess of a particular diastereconformer is higher in CHCl_3 solution. Although this reasoning is speculative, it is in reasonable agreement with NMR data (see previous section).

AM1 semiempirical calculations

The semiempirical calculations (AM1) were performed for derivatives of (*R*)-1-phenylethylamine (Fig. 8). The only simplification compared to real compounds consisted of using methyl, instead of iso-butyl or ethyl group at the lower rim of resorcin[4]arenes, which is believed to have a minor impact on the conformational preferences. In order to screen a conformational space for each compound KITE-(*M*), KITE-(*P*), VASE-(*M*) and VASE-(*P*) were preset (Fig. 8) and then for each conformation the torsion angles between the amide part and the benzylamine part ($T1$) were varied

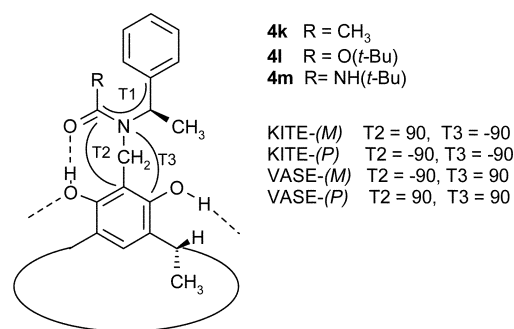


Fig. 8 Preset for AM1 optimizations.

by 30° and the resulting structures were optimized. The KITE conformations are obtained when the eight-membered ring points its N atom out from the molecular cavity ($T3 = -90^\circ$), while VASE conformations were generated by pre-setting the N atom to be directed inward ($T3 = 90^\circ$). During the optimization the torsion angles $T1$ underwent changes but a change from (*M*) to (*P*) configuration or *vice versa* was never observed.

Table 2 presents the results of the AM1 optimizations. Most optimized conformations have C_2 symmetry and the slightly flattened-cone conformation of the parent resorcin[4]arene ring. Although NMR and X-ray analysis shows the C_4 symmetry, the result of the calculations is not in contradiction since the interconversions between two C_2 conformations are probably facile, thus the time-averaged conformation has a C_4 symmetry.

For the least crowded acetyl derivative **4k** the AM1 calculations indicate that the VASE-(*M*) is most stable conformation. It should be noted that the number of low energy stable conformations is relatively larger than for **4i** and **4m**. This indicates that the flexibility of this system is considerably larger than for other derivatives.

For **4i** ((*R*)-phenylethylamine-Boc, an analogue of **4d** and **4e**), AM1 calculations gave predominately two conformations KITE-(*P*) and VASE-(*M*) (Table 2). The most stable KITE-(*P*) conformation is the only one with low energy among the KITE conformations. In fact NMR spectra for analogous compound **4e** suggested the presence of a single diastereconformer. The stability of the VASE-(*M*) conformation is rather surprising since it is tightly packed with all four methyl group closing the upper rim of the molecule. To double-check the result an extensive additional search for low energy KITE-**4i** conformations was performed (other dihedral angles were also varied and additionally non-symmetric conformations were also checked) but did not yield any conformation that was different from the one that was originally found.

For molecule **4m** ((*R*)-phenylethylamine-Bac, an analogue of compounds **4i** and **4j**), AM1 calculations gave two stable KITE cycloconformers: KITE-(*M*)-(*R*)-**4m** (68%) and KITE-(*P*)-(*R*)-**4m** (25%). Thus the calculations predicted higher stability of the *M*-cycloconformer *i.e.* the same as observed in the solid state for analogous compound **4j**. The diastereconformer ratio is also in rough agreement with the NMR data (for **4i** two diastereconformers were observed with ratio 86 : 14). However, it should be pointed out that in the case of the molecule having *tert*-butylaminocarbonyl substituents the most stable cycloenantiomer is the opposite to the one for the molecule with *tert*-butoxycarbonyl groups.

Table 2 Semiempirical AM1 optimization results

Comp.	Conformation	$T1_{\text{out}}/^\circ$	Relative energy/kcal mol ⁻¹	Distribution at 295 K
4k	VASE-(<i>M</i>)	-65, -75 (×3)	0	0.4486
	KITE-(<i>P</i>)	-68	0.53	0.1816
	VASE-(<i>M</i>)	-75	0.75	0.1248
	VASE-(<i>M</i>)	-93, -75 (×3)	1.07	0.0725
	VASE-(<i>M</i>)	-60	1.11	0.0681
	KITE-(<i>M</i>)	-60	1.15	0.0626
	KITE-(<i>M</i>)	-51	1.77	0.0209
	VASE-(<i>P</i>)	96	1.86	0.0188
	KITE-(<i>M</i>)	96	3.42	0.0013
	VASE-(<i>P</i>)	74	4.29	0.0002
	KITE-(<i>M</i>)	71	5.07	<0.0001
	VASE-(<i>P</i>)	98, -52, 72, -52	5.19	<0.0001
	VASE-(<i>P</i>)	-54	5.82	<0.0001
	KITE-(<i>P</i>)	74	6.57	<0.0001
	4l	KITE-(<i>P</i>)	-81	0
VASE-(<i>M</i>)		-81	0.03	0.4855
KITE-(<i>M</i>)		88	3.85	0.0007
VASE-(<i>P</i>)		86	2.79	0.0043
KITE-(<i>M</i>)		-71	5.52	<0.0001
KITE-(<i>P</i>)		92	9.84	<0.0001
4m	KITE-(<i>M</i>)	-60	0	0.6821
	KITE-(<i>P</i>)	-66	0.59	0.2484
	VASE-(<i>M</i>)	-64	1.34	0.0695
	VASE-(<i>P</i>)	-55	5.71	<0.0001
	VASE-(<i>P</i>)	66	9.23	<0.0001

It should be emphasized that the results of these calculations should be interpreted with great caution. Although it seems intuitive that the KITE conformations should be more stable due to the lack of steric overcrowding, the calculations suggest that the VASE conformations are not unthinkable, and even they can be quite stable. However, the internal volumes of the VASE conformations are very small and usually their “doors” at the upper rims are tightly closed.

Conclusions

The resorcinarenes **1a,b** can be conveniently transformed into upper rim amido substituted resorcin[4]arenes **4a–j** using a sequence of reactions: the Mannich reaction, removal of the *N,O*-acetal bridge and subsequent *N*-substitution with an RCO group. The newly discovered efficient procedure of *N,O*-acetal removal using ethyl nitroacetate is very mild as compared with the known procedure using refluxing in HCl and butanol. This may be advantageous for the synthesis of more sensitive compounds (*e.g.* hydrolysis-prone amino acid derivatives).

Amide substituted resorcin[4]arenes **4a–j** exist as conformational cycloisomers stabilized by belts of hydrogen bonds. The exchange between cycloconformers is slow on the NMR timescale. It allows for determination of the racemization barriers and relative stability of the cyclodiastereoisomers. Based on relatively high racemization barriers it can be concluded that the cycloisomerization process proceeds through simultaneous rupture of all eight hydrogen bonds. This is a quite surprising result assuming that the hydrogen bond system is spatially divided into four parts, *i.e.* each part consists of just two hydrogen bonds. However, rotation of just one unit creates an unfavourable pattern of the adjacent hydrogen bonds, which is enough to prevent stability (and detection) of such

intermediates and thus for racemization simultaneous rotation of all units is required.

Although these systems are not very promising for complexation due to their KITE conformations resulting in relatively shallow cavities, they offer an interesting insight into a restricted molecular motion of the propeller-like chiral molecules, which are of particular interest as molecular rotors.²⁵

Experimental

All chemicals were used as received unless otherwise noted. Reagent grade solvents (CH₂Cl₂, hexanes) were distilled prior to use. All reported ¹H NMR spectra were collected on a Bruker spectrometer at 500 (¹H NMR) and 125 (¹³C NMR) MHz. Chemical shifts are reported as δ values relative to the TMS signal defined at $\delta = 0.00$ (¹H NMR) or relative to the CDCl₃ signal defined at $\delta = 77.00$ (¹³C NMR). Mass spectra were obtained on a Mariner PerSeptive Biosystem instrument using the ESI technique. Chromatography was performed on silica gel (Kieselgel 60, 200–400 mesh).

The semiempirical calculations were performed using Gaussian 03 software.²⁶

CD spectroscopy

CD spectra were measured at room temperature in chloroform (for UV spectroscopy, Fluka) with solutions with concentrations of 1×10^{-4} M on a Jasco 715 spectrophotometer by using cells with path length 0.1 to 1 cm (spectral band width 2 nm, sensitivity 5×10^{-6} or 10×10^{-6} (ΔA -unit nm⁻¹), where $\Delta A = A_L - A_R$ is the difference in the absorbance). $\Delta \epsilon$ is expressed in units of L mol⁻¹ cm⁻¹.

NMR experiments

Variable temperature NMR spectra were recorded on a 500 MHz Bruker spectrometer equipped with a BTO2000 thermocouple. The spectra were recorded in such a way that the whole set of samples was recorded at a given temperature after stabilization at the same time (roughly).

The EXSY spectra were recorded at 303 K at 500 MHz on a Bruker spectrometer with a phase sensitive NOESY pulse sequence supplied with the Bruker software. The integration of the 2D spectra was preformed using XWin-NMR software. From the integrals of the cross-peaks and the diagonal peaks and mole fractions the rate constants were calculated according to known equations.²²

The general procedure for the Mannich reaction

Compounds **2a–d** were prepared following the known procedure with small modification. To a solution of resorcinarene **1**²⁷ (1 mmol), formaldehyde (37%, 0.75 ml, 10 mmol) and glacial acetic acid (0.5 ml) in methanol (5 ml), amine (5 mmol) was added. After 24 h at room temperature the precipitate was filtered off, washed with methanol and dried. All physicochemical properties of compounds **2a,b, e** and **2c,d**, concur with published data.^{10,12}

Procedure for *N*-substitution (steps b and c)

Method A. To a solution of tetrabezoxazine **2** (0.1 mmol) in 1 ml of methanol, ethyl nitroacetate was added (100 μ l). The solution was stirred for 2h. During that time the suspension dissolves and TLC shows substrate spot disappearance. To that solution 50 μ l of water was added and 200 mg of Boc₂O. The reaction was stirred overnight. The precipitate was filtered out and recrystallized from CH₂Cl₂/MeCN to give product **4**. The filtrate was checked by TLC for the presence of product, and if the product was detected in noticeable amount the filtrate was subjected to column chromatography on silica gel (eluent usually hexane:ethyl acetate 8:2). However, usually the product after chromatography was still contaminated with traces of ethyl nitroacetate, so recrystallization/precipitation was required to obtain analytically pure products. The additional portions obtained by chromatography did not exceed 10% yield.

Method B. To a solution of tetrabezoxazine **2** (0.1 mmol) in 1 ml of methanol, ethyl nitroacetate was added (100 μ l). The solution was stirred for 2 h. During that time the suspension dissolves and TLC shows substrate spot disappearance. The solution was then evaporated at reduced pressure (30 °C, water bath) and vacuum dried. The resulting oil was washed with hexane (3 \times 2 ml) and dried again. The oil was dissolved in 2 ml of dry THF and then 60 μ l of *tert*-butyl isocyanate was added. The reaction was stirred overnight. The mixture was then treated with 1 ml of methanol in order to decompose the remaining isocyanate and evaporated. Crude product **4** was purified by column chromatography on silica gel using hexane–AcOEt (8 : 2) and additionally recrystallized/precipitated from CH₂Cl₂/MeCN.

4a. Method A, yield 56%. δ_{H} (500 MHz, CDCl₃, TMS, 303 K): 0.96 (d, $J = 10.0$ Hz, 12 H, H_{a}), 0.99 (d, $J = 10.0$ Hz, 12 H, H_{a}), 1.49 (bs, 4 H, H_{b}), 2.08 (bs, 20 H, H_{c} , H_{acetyl}), 4.10–5.20 (bm, 20H, H_{f} , H_{d} , H_{g}), 7.20–7.34 (m, 24 H, H_{ar}), 8.68 (bs, 4 H, OH), 11.40 (bs,

4 H, OH). δ_{C} (125 MHz, CDCl₃, 303 K): 22.85, 22.96, 26.68, 31.75, 42.09 (br), 42.80, 53.01, 111.65, 123.67, 124.66, 126.39, 127.46, 128.85, 136.53, 150.25, 151.72, 173.91. ESI MS m/z Calcd for [C₈₄H₁₀₀N₄O₁₂ – H][–] 1355.7; found 1355.7, isotope profile agrees. Anal. Calcd for C₉₆H₁₂₈N₄O₁₆: C 74.31, H 7.42, N 4.13%; found C 74.15, H 7.32, N 4.30%.

4b. Method A, yield 99%. δ_{H} (500 MHz, CDCl₃, TMS, 303 K): 0.98 (m, 24 H, H_{a}), 1.25–1.45 (bs, 36 H, C(CH₃)₃), 1.51 (m, 4H, H_{b}), 2.10 (bs, 8H, H_{c}), 4.20–4.75 (bm, 20H, H_{f} , H_{d} , H_{g}), 7.20–7.28 (m, 24H, H_{ar}), 8.65 (bs, 4 H, OH), 11.04 (bs, 4 H, OH). δ_{C} (125 MHz, CDCl₃, 303K): 22.76, 22.76, 26.11, 27.42, 28.26, 31.80, 40.5 (br), 42.90, 50.83, 81.64, 112.21, 123.56, 124.49, 124.83, 126.94, 127.62, 128.29, 138.47, 150.29, 151.63, 158.78. ESI MS m/z Calcd for [C₉₆H₁₂₈N₄O₁₆Na]⁺ 1611.9; found 1612.0, isotope profile agrees. Anal. Calcd for C₉₆H₁₂₈N₄O₁₆: C 72.33, H 8.09, N 3.51%; found C 72.23, H 7.92, N 3.68%.

4c. Method A, yield 61%. δ_{H} (500 MHz, CDCl₃, TMS, 303 K): 0.91 (t, $J = 7.3$ Hz, 12 H, CH₂–CH₃), 0.96 (d, $J = 6.5$ Hz, 24 H, H_{a}), 1.29 (m, 4H, H_{b}), 1.32–1.52 (m, 52 H, CH₂, C(CH₃)₃), 2.02 (bs, 8H, H_{c}), 3.32 (bs, 8H, N–CH₂), 4.31 (bm, 8 H, $H_{\text{f},2}$), 4.53 (bt, 4 H, H_{d}), 7.17 (s, 4H, H_{ar}), 8.50 (bs, 4 H, OH), 10.93 (bs, 4 H, OH). δ_{C} (125 MHz, CDCl₃, 303 K): 13.86, 19.98, 22.83, 26.16, 27.47, 28.43, 30.35, 31.85, 40.92, 43.10, 47.36, 80.88, 112.45, 123.51, 124.38, 124.74, 150.26, 151.65, 158.79. ESI MS m/z Calcd for [C₈₄H₁₃₂N₄O₁₆Na]⁺ 1476.0, found 1476.0, isotope profile agrees.

4d. Method A, yield 56%. $[\alpha]_{\text{D}} = +93.3$ (c 1.13, CHCl₃). δ_{H} (500 MHz, CDCl₃, TMS, 303 K): 0.90 (bd, 12 H, H_{a}), 0.96 (d, $J = 6.6$ Hz, 12 H, H_{a}), 1.52 (m, 4H, H_{b}), 1.64 (bs, 12H, H_{b}), 2.11 (bm, 8H, H_{c}), 4.50–4.56 (m, 12H, H_{f} , H_{d}), 5.10, (q, $J = 6.8$ Hz, 4H, H_{g}), 7.01 (m, 8H, H_{ar}), 6.98–7.25 (m, 24H, H_{ar}), 8.54 (bs, 4 H, OH), 10.96 (bs, 4 H, OH). δ_{C} (125 MHz, CDCl₃, 303 K): 16.12 (br), 22.67, 22.78, 26.29, 27.42, 28.01, 31.76, 42.78, 43.15 (br), 56.73, 81.41, 112.24, 123.71, 124.52, 124.65, 126.09, 126.37, 127.51, 142.71, 150.11, 151.41, 158.51. ESI MS m/z Calcd for [C₁₀₀H₁₃₂N₄O₁₆H]⁺ 1646.0, found 1646.5, isotope profile agrees.

4e. Method A, yield 56%. $[\alpha]_{\text{D}} = +140.4$ (c 1.19, CHCl₃). δ_{H} (500 MHz, CDCl₃, TMS, 303 K): 0.94 (t, $J = 7.0$ Hz, 12 H, H_{a}), 1.10 (s, 36 H, H_{f}), 1.52 (m, 4H, H_{b}), 1.64 (bs, 12H, H_{b}), 2.27 (m, 8H, H_{b}), 4.33 (m, 4 H, H_{d}), 4.49 (AB/2, $J_{\text{AB}} = 20.9$ Hz, 4 H, $H_{\text{f},1}$), 4.54 (AB/2, $J_{\text{AB}} = 20.9$ Hz, 4H, $H_{\text{f},2}$), 5.08 (q, $J = 6.8$, 4 H, H_{g}), 6.99–7.06 (m, 20H, H_{f}), 7.26 (s, 4 H, H_{c}), 8.57 (bs, 4 H, OH), 10.89 (bs, 4 H, OH). δ_{C} (125 MHz, CDCl₃, 303 K): 26.84, 28.05, 36.27, 43.12, 56.67, 81.34, 112.21, 123.19, 124.46, 124.54, 126.13, 126.46, 127.59, 142.77, 150.23, 151.60, 158.52. ESI MS m/z Calcd for [C₉₂H₁₁₆N₄O₁₆Na]⁺ 1555.8, found 1555.8, isotope profile agrees. Anal. Calcd for C₉₂H₁₁₆N₄O₁₆·0.5 CH₃CN·0.5 CH₂Cl₂: C 70.32, H 7.48, N 3.84%; found C 70.40, H 7.39, N 4.00%.

4f. Method B, yield 63%. δ_{H} (500 MHz, CDCl₃, TMS, 303 K): 0.94 (d, $J = 6.6$ Hz, 12 H, H_{a}), 0.98 (d, $J = 6.6$ Hz, 12 H, H_{a}), 1.08 (s, 36 H, C(CH₃)₃), 1.53 (q, $J = 6.6$ Hz, 4H, H_{b}), 2.11 (bs, 8H, H_{c}), 4.18 (s, 4 H, NH), 4.35–4.95 (bm, 20H, H_{f} , H_{d} , H_{g}), 7.15 (bd, 8H, $J = 7.0$ Hz, H_{ar}), 7.22–7.29 (m, 16H, H_{ar}), 8.77 (bs, 4 H, OH), 12.04 (bs, 4 H, OH). δ_{C} (125 MHz, CDCl₃, 303 K): 22.79, 22.88, 26.15, 29.08, 31.78, 42.83, 51.09, 51.77, 112.67, 123.35, 124.58, 126.38, 127.40, 128.85, 137.43, 150.59, 151.64, 159.62. $\delta_{\text{N}} = -273.8$ ppm (NH). ESI MS m/z Calcd for [C₉₆H₁₂₈N₈O₁₂Na]⁺ 1607.9; found 1608.0, isotope profile agrees.

4g. Method B, yield 25%. δ_{H} (500 MHz, CDCl₃, TMS, 303 K): 0.97 (t, $J = 7.1$ Hz, 12 H, CH₂–CH₃), 1.11 (s, 36 H, C(CH₃)₃),

2.28 (m, 8H, CH₂-CH₃), 4.22 (s, 4 H, NH), 4.36 (bt, 4 H, H_a), 4.43–4.95 (bm, 16H, H_f, H_g), 7.18–7.32 (m, 24H, H_{ar}), 8.82 (bs, 4 H, OH), 12.04 (bs, 4 H, OH). δ_c (125 MHz, CDCl₃, 303 K): 12.71, 26.72, 29.11, 36.33, 42.56 (br), 51.09, 51.69, 112.66, 122.90, 124.42, 124.55, 126.38, 127.41, 128.87, 137.41, 150.65, 151.78, 159.63. ESI MS *m/z* Calcd for [C₈₈H₁₁₂N₈O₁₂Na]⁺ 1495.8; found 1495.9, isotope profile agrees. Anal. Calcd for C₈₈H₁₁₂N₈O₁₂·0.7 CH₃CN·0.3 CH₂Cl₂ C 70.50, H 7.56, N 7.97%; found C 70.48, H 7.35, N 8.07%.

4h. Method B, yield 54%. δ_H (500 MHz, CDCl₃, TMS, 303 K): 0.93–0.96 (m, 36 H, CH₂-CH₃, H_a), 1.29 (m, 4H, H_b), 1.32 (s, 36 H, C(CH₃)₃), 1.26–1.37 (m, 12 H, CH₂, H_b), 1.47–1.53 (m, 16 H, CH₂), 2.06 (bs, 8H, H_c), 3.13 (bs, 4H, N-CH₂), 3.32 (bs, 4H, N-CH₂), 4.24 (bm, 8 H, NH, H_{f1}), 4.38 (d, *J* = 14.6 Hz, 4 H, H_{f2}), 4.53 (t, *J* = 7.9 Hz, 4 H, H_d), 7.15 (s, 4H, H_{ar}), 8.71 (bs, 4 H, OH), 11.94 (bs, 4 H, OH). δ_c (125 MHz, CDCl₃, 303 K): 13.87, 20.29, 22.82, 22.87, 26.17, 29.54, 30.08, 31.85, 40.73, 43.06, 47.48, 51.08, 112.66, 123.28, 124.46, 150.70, 151.65, 159.28. ESI MS *m/z* Calcd for [C₈₄H₁₃₆N₈O₁₂Na]⁺ 1472.0; found 1472.0, isotope profile agrees.

4i. Method B, yield 48%. [α]_D = +137.5 (*c* 1.13, CHCl₃). Main diastereoconformer (86%): δ_H (500 MHz, CDCl₃, TMS, 303 K): 0.91 (m, 48 H, H_a, H_j), 0.97 (d, *J* = 6.4 Hz, 12 H, H_a), 1.54 (m, 4H, H_b), 1.62 (bs, 12H, H_b), 2.11 (m, 8H, H_c), 3.94 (s, 4 H, NH), 4.45 (bs, 4H, H_{f1}), 4.59 (bt, 4 H, H_d), 4.65 (d, *J* = 14.6 Hz, 4H, H_{f2}), 5.35 (q, *J* = 6.8 Hz, 4H, H_g), 7.01 (m, 8H, H_i), 7.21–7.25 (m, 16H, H_e, H_i), 8.75 (bs, 4 H, OH), 11.90 (bs, 4 H, OH). δ_c (125 MHz, CDCl₃, 303 K): 15.21, 22.65, 22.82, 26.35, 28.92, 31.79, 42.64, 43.57, 50.90, 56.02, 112.92, 123.42, 124.64, 126.25, 127.39, 128.67, 141.38, 150.45, 151.51, 158.49. δ_N –269.1 ppm (NH). ESI MS *m/z* Calcd for [C₁₀₀H₁₃₆N₈O₁₂Na]⁺ 1664.0, found 1664.0, isotope profile agrees. Anal. Calcd for C₁₀₀H₁₃₆N₈O₁₂ C 73.14, H 8.35, N 6.82%; found C 73.02, H 8.54, N 6.84%. Minor diastereoconformer (14%, well separated signals only) δ_H (500 MHz, CDCl₃, TMS): 1.49 (m, 4H, H_b, H_h), 1.90 (bm, 8H, H_c), 4.02 (s, 4 H, NH), 8.77 (bs, 4 H, OH), 12.00 (bs, 4 H, OH). δ_c (125 MHz, CDCl₃, TMS): 22.50, 22.97, 29.03, 56.55, 124.44, 126.25, 128.86, 158.75.

4j. Method B, yield 30%. [α]_D = +145.3 (*c* 1.14, CHCl₃). Main diastereoconformer (84%): δ_H (500 MHz, CDCl₃, TMS, 303 K): 0.95 (m, 48 H, H_a, H_j), 1.64 (bs, 12H, H_b), 2.30 (bs, 8H, H_b), 3.96 (s, 4 H, NH), 4.37–4.68 (m, 12H, H_{f1,2}, H_d), 5.35 (q, *J* = 6.0 Hz, 4H, H_g), 7.11–7.26 (m, 24 H, H_{ar}), 8.79 (bs, 4 H, OH), 11.88 (bs, 4 H, OH). δ_c (125 MHz, CDCl₃, 303 K): 12.47, 15.22, 26.69, 28.95, 29.06, 36.30, 43.45, 50.88, 55.87, 112.83, 122.88, 124.55, 126.51, 127.40, 128.72, 141.43, 150.58, 151.68, 158.48. ESI MS *m/z* Calcd for [C₉₂H₁₂₀N₈O₁₂H]⁺ 1529.9; found 1529.9, isotope profile agrees. Anal. Calcd for C₉₂H₁₂₀N₈O₁₂·0.6 CH₃CN·0.4 CH₂Cl₂ C 70.77, H 7.78, N 7.58%; found C 70.92, H 7.80, N 7.63%. Minor diastereoconformer (16%, well separated signals only) δ_H (500 MHz, CDCl₃, TMS): 1.51 (m, 4H, H_b), 4.04 (s, 4 H, NH), 8.91 (bs, 4 H, OH), 12.00 (bs, 4 H, OH). δ_c (125 MHz, CDCl₃, TMS): 29.06, 56.50, 124.36, 126.30, 128.86, 158.70.

X-Ray crystallographic structure determination of 4j

The diffraction quality crystals were grown from CH₂Cl₂/MeCN solution. The measurement was performed on a KM4CCD κ -axis diffractometer with graphite-monochromated MoK α radiation. The crystal was positioned at 62 mm from the CCD camera. 1500

Frames were measured at 0.5° intervals with a counting time of 30 se. The data were corrected for Lorentz and polarization effects. Empirical correction for absorption was applied. Data reduction and analysis were carried out with the Oxford Diffraction programs. The structure was solved by direct methods and refined using SHELXL (X-Seed²⁸ interface). The refinement was based on *F*² for all reflections except those with very negative *F*². Weighted *R* factors *wR* and all goodness-of-fit *S* values are based on *F*². The non-hydrogen atoms were refined with anisotropic thermal parameters, the H atoms attached to carbon atoms were positioned geometrically. The OH hydrogen atoms were located from the Fourier map and then refined with restraints on the bond lengths only.

Crystal data for **4j**: C_{94.69}H_{126.10}N_{8.65}O_{13.38} (**4j**·(CH₃CN)_{0.65}·(CH₂Cl₂)_{0.35}), *M* = 1599.53, tetragonal, space group *I4* (no. 79), *a* = *b* = 23.3843(6), *c* = 8.2561(2) Å, *V* = 4514.6(2) Å³, *Z* = 2, *D*_c = 1.177 g cm⁻³, *F*₀₀₀ = 1724, MoK α radiation, λ = 0.71073 Å, *T* = 173(2)K, $2\theta_{\max}$ = 57.4°, 21498 reflections collected, 4767 unique (*R*_{int} = 0.0378). Final GooF = 0.776, *R*₁ = 0.0468, *wR*₂ = 0.1182, *R* indices based on 1993 reflections with *I* > 2σ(*I*) (refinement on *F*²), 279 parameters, 3 restraints. Lp and absorption corrections applied, μ = 0.078 mm⁻¹. Absolute structure parameter = 1.2(16).

CCDC reference number 635229. For crystallographic data in CIF or other electronic format see DOI: 10.1039/b701451a

Acknowledgements

This work was supported by the State Committee for Scientific Research (Project # N204 086 31/2028). I am grateful to Prof. Sławomir Szymański for his valuable insights concerning NMR experiments and data interpretation, Michał Gałęzowski for SPARTAN calculations and Dr Dorota Gryko for HPLC experiments. The X-ray measurements were undertaken in the Crystallographic Unit of the Physical Chemistry Lab. at the Chemistry Department of the University of Warsaw

References

- 1 Y. Fukushi, *Nippon Nogei Kagaku Kaishi*, 1998, **72**, 1345–1351; Y. Fukushi, K. Shigematsu, J. Mizutani and S. Tahara, *Tetrahedron Lett.*, 1996, **37**, 4737–4740; X. Borde, C. Nugier-Chauvin, H. Noiret and N. Patin, *Tetrahedron: Asymmetry*, 1998, **9**, 1087–1090; M. J. Ferreiro, S. K. Latypov, E. Quinoa and R. Riguera, *Tetrahedron: Asymmetry*, 1997, **8**, 1015–1018; M. J. Ferreiro, S. K. Latypov, E. Quinoa and R. Riguera, *Tetrahedron: Asymmetry*, 1996, **7**, 2195–2198.
- 2 A. V. Malkov and P. Kocovsky, *Curr. Org. Chem.*, 2003, **7**, 1737–1757; H. U. Blaser and C. Malan, *Adv. Synth. Catal.*, 2003, **345**, 103–151; B. Pugin, F. Spindler, H. Steiner, M. Studer and M. Nakajima, *Yakugaku Zasshi*, 2000, **120**, 68–75; T. T. L. Au-Yeung and A. S. C. Chan, *Coord. Chem. Rev.*, 2004, **248**, 2151–2164.
- 3 T. Focken, G. Raabe and C. Bolm, *Tetrahedron: Asymmetry*, 2004, **15**, 1693–1706; R. C. J. Atkinson, V. C. Gibson and N. J. Long, *Chem. Soc. Rev.*, 2004, **33**, 313–328.
- 4 A. D. Cort, J. I. M. Murua, C. Pasquini, M. Pons and L. Schiaffino, *Chem.–Eur. J.*, 2004, **10**, 3301–3307.
- 5 F. Fabris, L. Pellizzaro, C. Zonta and O. De Lucchi, *Eur. J. Org. Chem.*, 2007, 283–291.
- 6 A. D. Cort, L. Mandolini, C. Pasquini and L. Schiaffino, *New J. Chem.*, 2004, **28**, 1198–1199.
- 7 Cycloenantiomerism was first discussed in the case of cyclopeptides and catenanes: V. Prelog and H. Gerlach, *Helv. Chim. Acta*, 1964, **47**, 2288–2294; M. D. G. Schill, *Catenanes, Rotaxanes, and Knots*, Academic Press, New York, 1971, pp. 11–15; C. Reuter, R. Schmieder and F. Vogtle, *Pure Appl. Chem.*, 2000, **72**, 2233–2241.

- 8 M. D. Singh, J. Siegel, S. E. Biali and K. Mislow, *J. Am. Chem. Soc.*, 1987, **109**, 3397–3402; K. Mislow, *Chimia*, 1986, **40**, 395–402.
- 9 V. Böhmer, D. Kraft and M. Tabatabai, *J. Inclusion Phenom. Mol. Recognit. Chem.*, 1994, **19**, 17–39.
- 10 R. Arnecke, V. Böhmer, E. F. Paulus and W. Vogt, *J. Am. Chem. Soc.*, 1995, **117**, 3286–3287.
- 11 P. C. B. Page, H. Heaney and E. P. Sampler, *J. Am. Chem. Soc.*, 1999, **121**, 6751–6752; M. Klaes, C. Agena, M. Kohler, M. Inoue, T. Wada, Y. Inoue and J. Mattay, *Eur. J. Org. Chem.*, 2003, 1404–1409.
- 12 W. Iwanek and J. Mattay, *Liebigs Ann. Chem.*, 1995, 1463–1466; M. T. El Gihani, H. Heaney and A. M. Z. Slawin, *Tetrahedron Lett.*, 1995, **36**, 4905–4908; R. Arnecke, V. Böhmer, S. Friebe, S. Gebauer, G. J. Krauss, I. Thondorf and W. Vogt, *Tetrahedron Lett.*, 1995, **36**, 6221–6224; A. Szumna, M. Gorski and O. Lukin, *Tetrahedron Lett.*, 2005, **46**, 7423–7426.
- 13 O. Trapp, S. Caccamese, C. Schmidt, V. Böhmer and V. Schurig, *Tetrahedron: Asymmetry*, 2001, **12**, 1395–1398.
- 14 D. M. Rudkevich, G. Hilmersson and J. Rebek, *J. Am. Chem. Soc.*, 1997, **119**, 9911–9912.
- 15 S. Saito, C. Nuckolls and J. Rebek, *J. Am. Chem. Soc.*, 2000, **122**, 9628–9630.
- 16 A. Shivanyuk, K. Rissanen, S. K. Korner, D. M. Rudkevich and J. Rebek, *Helv. Chim. Acta*, 2000, 831778–1790.
- 17 O. Hayashida, S. Matsumoto and I. Hamachi, *Chem. Lett.*, 2005, **34**, 1276–1277; O. Hayashida, J. Ito, S. Matsumoto and I. Hamachi, *Org. Biomol. Chem.*, 2005, **3**, 654–660.
- 18 L. Frkanec, A. Visnjevac, B. Kojic-Prodic and M. Zinic, *Chem.–Eur. J.*, 2000, **6**, 442–453.
- 19 C. Schmidt, E. F. Paulus, V. Böhmer and W. Vogt, *New J. Chem.*, 2000, **24**, 123–125.
- 20 S. V. Chankeshwara and A. K. Chakraborti, *Org. Lett.*, 2006, **8**, 3259–3262.
- 21 B. R. Buckley, J. Y. Boxhall, P. C. B. Page, Y. Chan, M. R. J. Elsegood, H. Heaney, K. E. Holmes, M. J. McIldowie, V. McKee, M. J. McGrath, M. Mocerino, A. M. Poulton, E. P. Sampler, B. W. Skelton and A. H. White, *Eur. J. Org. Chem.*, 2006, 5117–5134.
- 22 C. L. Perrin and T. J. Dwyer, *Chem. Rev.*, 1990, **90**, 935–967.
- 23 J. Sartorius and H. J. Schneider, *Chem.–Eur. J.*, 1996, **2**, 1446–1452.
- 24 C. Schiel, G. A. Hembury, V. V. Borovkov, M. Klaes, C. Agena, T. Wada, S. Grimme, Y. Inoue and J. Mattay, *J. Org. Chem.*, 2006, **71**, 976–982.
- 25 G. S. Kottas, L. I. Clarke, D. Horinek and J. Michl, *Chem. Rev.*, 2005, **105**, 1281–1376.
- 26 M. J. Frisch, G. W. Trucks, H. B. Schlegel, G. E. Scuseria, M. A. Robb, J. R. Cheeseman, J. A. Montgomery, Jr., T. Vreven, K. N. Kudin, J. C. Burant, J. M. Millam, S. S. Iyengar, J. Tomasi, V. Barone, B. Mennucci, M. Cossi, G. Scalmani, N. Rega, G. A. Petersson, H. Nakatsuji, M. Hada, M. Ehara, K. Toyota, R. Fukuda, J. Hasegawa, M. Ishida, T. Nakajima, Y. Honda, O. Kitao, H. Nakai, M. Klene, X. Li, J. E. Knox, H. P. Hratchian, J. B. Cross, V. Bakken, C. Adamo, J. Jaramillo, R. Gomperts, R. E. Stratmann, O. Yazyev, A. J. Austin, R. Cammi, C. Pomelli, J. Ochterski, P. Y. Ayala, K. Morokuma, G. A. Voth, P. Salvador, J. J. Dannenberg, V. G. Zakrzewski, S. Dapprich, A. D. Daniels, M. C. Strain, O. Farkas, D. K. Malick, A. D. Rabuck, K. Raghavachari, J. B. Foresman, J. V. Ortiz, Q. Cui, A. G. Baboul, S. Clifford, J. Cioslowski, B. B. Stefanov, G. Liu, A. Liashenko, P. Piskorz, I. Komaromi, R. L. Martin, D. J. Fox, T. Keith, M. A. Al-Laham, C. Y. Peng, A. Nanayakkara, M. Challacombe, P. M. W. Gill, B. G. Johnson, W. Chen, M. W. Wong, C. Gonzalez and J. A. Pople, *GAUSSIAN 03 (Revision B.05)*, Gaussian, Inc., Pittsburgh, PA, 2003.
- 27 L. M. Tunstad, J. A. Tucker, E. Dalcanales, J. Weiser, J. A. Bryant, J. C. Sherman, R. C. Helgeson, C. B. Knobler and D. J. Cram, *J. Org. Chem.*, 1989, **54**, 1305–1312.
- 28 L. J. Barbour, *J. Supramol. Chem.*, 2001, **1**, 189–191.